



HAL
open science

Stability assessment of Con Dao Island grid with high penetration of photovoltaic systems

Quoc Tuan Tran, Tran The Hoang, Manh Hung Tran, Thang D. Nguyen, Viet Q. Nguyen

► **To cite this version:**

Quoc Tuan Tran, Tran The Hoang, Manh Hung Tran, Thang D. Nguyen, Viet Q. Nguyen. Stability assessment of Con Dao Island grid with high penetration of photovoltaic systems. IEEE PES General Meeting, Jul 2022, Denver, United States. pp.10.1109/PESGM48719.2022.9916978, 10.1109/PESGM48719.2022.9916978 . cea-04119795

HAL Id: cea-04119795

<https://cea.hal.science/cea-04119795>

Submitted on 6 Jun 2023

HAL is a multi-disciplinary open access archive for the deposit and dissemination of scientific research documents, whether they are published or not. The documents may come from teaching and research institutions in France or abroad, or from public or private research centers.

L'archive ouverte pluridisciplinaire **HAL**, est destinée au dépôt et à la diffusion de documents scientifiques de niveau recherche, publiés ou non, émanant des établissements d'enseignement et de recherche français ou étrangers, des laboratoires publics ou privés.

Stability Assessment of Con Dao Island Grid with High Penetration of Photovoltaic Systems

Quoc Tuan Tran, *Senior Member IEEE*, Tran The Hoang

University of Grenoble-Alpes, CEA-Liten, INES, 73375 Le Bourget-du-Lac, France

QuocTuan.Tran@cea.fr; tran-the.hoang@cea.fr

Abstract—The integration renewable energy sources, characterized by inherently intermittent characteristics and low inertia, into grids introduce several impacts on the network operation such as stability, protection and challenges for management. In this paper, the stability of Con Dao Island grid in Vietnam with high renewable energy penetration, especially photovoltaic (PV) and Wind Turbine (WT) energy, is extensively studied. The main purpose of this paper is to investigate the impacts of high renewable energy integration on stability of this grid. Then, several solutions to the stability issues, including Fault Ride Through (FRT) capability of PV system and implementation of battery, is proposed and validated. Numerous scenarios are considered, including different PV penetration levels (inertia impact) and different events (short circuits and generator outage). The results obtained show the significant impact of PV penetration levels on the grid stability. However, the proposed solutions demonstrate their high effectiveness in addressing the identified instability issues of the grids.

Index Terms—Island grid, Photovoltaic systems, Wind power, BESS, Stability, PV penetration, Short circuit, Diesel outage.

I. INTRODUCTION

The integration of renewable energy, characterized by inherently intermittent characteristics and low inertia, into grids have several impacts on the network operation such as stability, protection and challenges for management [1]–[15]. These impacts are more complicated for island or weak grids.

In contrast to utility or facility grids, an island grid is never connected to utility networks and its operation is normally controlled in a decentralized manner [4]. Power balancing in such kind of grid is usually taken over by, either small-size diesel generators or low-inertia inverter-interfaced sources such as photovoltaic (PV), wind turbine (WT), battery energy storage system (BESS), with limited spinning reserve and reactive power support. Ensuring transient stability of these grids after large disturbances is rather challenging and thus, requires comprehensive investigations. In [5], a thorough analysis on various issues related to the microgrid stability was presented. A mathematical modelling and stability assessment of an isolated microgrid was reported in [6]. Likewise, a distributed framework for stability evaluation and enhancement of inverter-based microgrids was designed in [7] while dynamic stability examination-based method based on eigenvalue sensitivity was fully developed in [8], [9]. Besides, authors in [10] stability and eigenvalue

sensitivity analysis of a BESS in a microgrid was presented with a high detail.

On the other hand, a variety of papers focusing on improvement of stand-alone grids has been recently published. For instance, paper in [11] deployed responsive charging electric vehicles and supplementary controller, whose control actions were directed by two Proportional-Derivative (PD) fuzzy logic, for enhancing the stability of an islanded microgrid. A similar approach utilizing a nonlinear supplementary controller for transient response improvement has been achieved in [12]. Intelligent fuzzy control was also adopted for guaranteeing autonomous microgrids [13]. An adaptive auto-reclosing scheme for preserving the microgrid transient stability was also taken into consideration in [14]. More interestingly, the impact of fault ride through (FRT) requirement applicable for inverter-interfaced generators imposed by new grid codes was analyzed and several solutions were suggested [15].



Figure 1. Côn Đảo Island district [Source: maps.google.com]

In this paper, the authors aim to perform an in-depth transient stability of an island grid supplying Con Dao Island district, which belongs to Ba Ria-Vung Tau province, Vietnam as shown in Fig. 1. The Con Dao Island district consists of 16 islands of various sizes and is situated around 185 km from Vung Tau city and 230 km from Ho Chi Minh City. The district covers an area of 76.7 km², out of which Con Son Island is the largest area with 51.51 km² wide where most of the socio-economic activities of district take place.

As a remote island district, electricity supply for Con Dao district relies primarily on diesel fuel that often suffer from high transportation cost over long distances from the mainland of Vietnam. Therefore, the generation cost of the region is rather high, ranging from 36 to 38 U.S. cents per kilowatt-hour compared to a national average number of 5.2 U.S. cent per kilowatt-hour. To reduce such a high generation cost, an interconnection with the national grid by constructing new undersea cables is being studied. However, the solution appears irrelevant in the context of the abundant capacity of wind and solar energies on Con Dao district given the significant reduction in the implementation cost of PV and WT plants. A more appropriate strategy in cost reduction is to increase the integration of PV and WT sources.

However, as indicated in many studies, the integration of renewable energies into the island grids is limited by the frequency instability margin. The higher penetration of these sources, the lower the overall grid inertia and thus many challenges not only to the grid stability but also to grid protection and management will arise. As is evident, in order to attain a high integration of PV and WT sources into Con Dao grid while ensuring its transient stability, the works done in this study are as follows:

- Investigate the impacts of integration of renewable energy, in particular, PV and WT sources, on the transient stability of Con Dao grid;
- Validate the effectiveness of several solutions for enhancing the stability of Con Dao grid such as FRT capability of PV systems or frequency control function provided by BESS.

Besides, the study is performed by considering the following factors: PV penetration level, BEES in role of the slack bus, and type of disturbances including short circuits and generator outage. The paper is structured as follows. The detailed description of Con Dao grid is provided in Section II. Different scenarios for transient stability of the grid are defined in Section III. Furthermore, simulation results are presented and discussed in Section IV and the conclusion is drawn in Section V.

II. DETAILED DESCRIPTION OF CON DAO GRID

Con Dao Power Grid (Fig. 2) is an island microgrid, being operated separately from the national grid. It is operating at two voltage levels including a medium voltage (MV) at 22 kV and low voltage (LV) at 0.4 kV.

There are three radial MV feeders originated from the 22 kV Busbar systems of the An Hoi power plant, supplying various single-phase and three-phase LV loads. Feeder 1 and Feeder 2 are meshed at several points by normally open switches. The total length of MV feeders in the district is 51.5 km, including 5.5 km of single-phase lines (accounting for 12.5%), and 46 km of three-phase lines. The grounding system is the solidly and undistributed method.

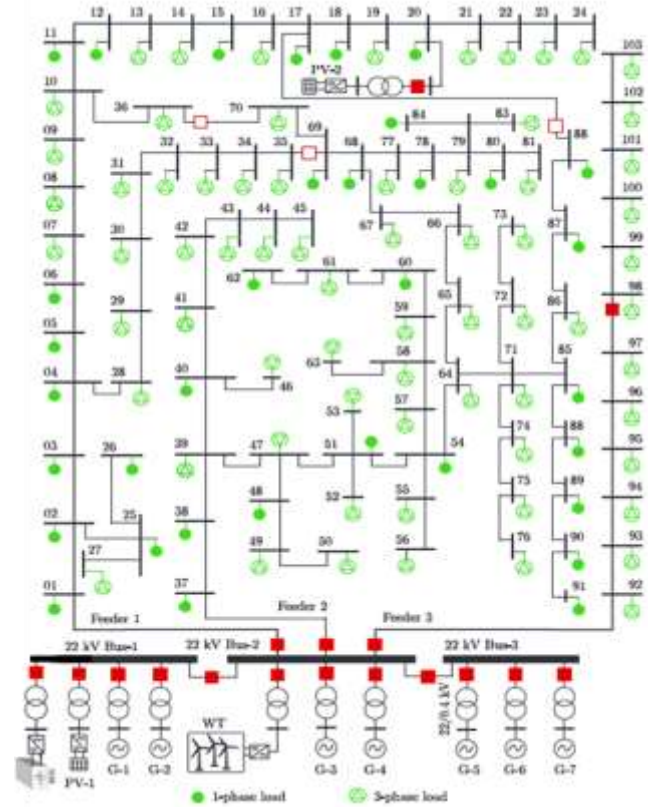


Figure 2. Single-line diagram of Con Dao Grid

A. Loads

Since the grid daily consumption pattern is rather similar throughout a year, only a daily load profile in 2020 presented in Fig. 3 is considered. The maximal loading level is 7 MW. Another striking feature is that Con Dao Grid consists of both three-phase and single-phase loads at 22 kV level.

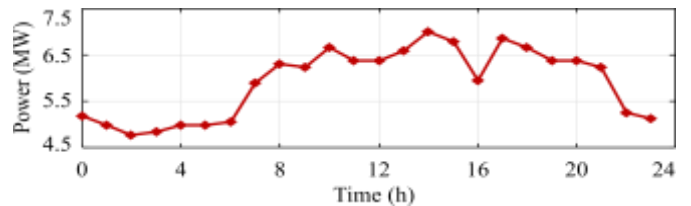


Figure 3. Profile of daily load

B. Generation

Seven diesel generators are installed at the An Hoi power plant (Fig. 2) with Cummins (G1-G4), Perkins (G5) and Caterpillar (G6-G7), each with the rated power of 1.5 MW. There are two PV power plants with PV1 of 1.5 MW rating being installed at Bus 1 of the An Hoi power plant and PV2 of 1 MW rating being connected at Bus 20. Besides, a wind power plant of 3 MW rating is also installed at Bus 2 of the An Hoi power plant (Bus 2, Fig. 1).

C. Storage system

A BESS is connected at the An Hoi power plant (Bus 1) with a capacity of 5MWh and rated power of 5MW. This BESS is capable of controlling the grid frequency in role of a master when required. This control mode of the BESS is derived from the component library provided by PowerFactory.

III. STUDY SCENARIOS

To approximately determine the maximum level of PV penetration that Con Dao grid can tolerate while ensuring its transient stability, different scenarios with PV penetration level varying from 0 up to 60% of the total grid generation by a step of 15% are considered. In the study, for simplify the WT capacity is left constant. This assumption does not affect the generality of the conducted study on the impact of renewable energy on the grid stability since both PV and WT sources are coupled with the grid through power electronic converters with inherent nature of low inertia. In addition to variation of PV level, different types of disturbance are also taken into consideration including short circuit on MV feeders and loss of a diesel generator. In the following, two cases with different sub-scenarios are specified.

Table 1: Proportion of different sources with estimated system inertia

| PV level | Diesel | PV, (MW) | WT (MW) | PV + WT Rate (%) | H_{sys} (s) |
|----------|--------|----------|---------|------------------|---------------|
| PV0% | G1-G6 | 0 | 1.5 | 21.4 | 4.82 |
| PV15% | G1-G5 | 1.05 | 1.5 | 32.1 | 4.02 |
| PV30% | G1-G4 | 2.1 | 1.5 | 51.4 | 3.21 |
| PV45% | G1-G3 | 3.15 | 1.5 | 66.4 | 2.41 |
| PV60% | G1-G2 | 4.2 | 1.5 | 81.4 | 1.61 |

Case A: Diesel G1 plays a role of slack bus with disturbances being short circuits and PV penetration varying from 0 to 60%. Two sub-scenarios are as follows:

- PVs without FRT capability;
- PVs capable of providing FRT capability.

The PV penetration ratio is calculated as the ratio of total PV capacity to total load capacity. The calculation for a total load consumption of 7 MW used for the scenario is provided in Table 1. For varying the PV penetration level, each PV power plant is assumed to consist of a number of PV systems up to 12 units with a rating of 350 kWp each.

Case B: BESS plays the role of slack bus with disturbances being either short circuit or loss of a unit. Moreover, when diesel generator G1 is lost, the grid will have a renewable penetration of 100%.

For these above two study cases, short circuits are either single or three-phase short circuit occurring at Feeder 2, on the line section between N38 and N39 (Fig. 2). The short circuit take place at 2 s and then is eliminated at 2.15 s owing to the disconnection of feeder 2.

IV. SIMULATION RESULTS AND DISCUSSION

A. Case A: Diesel generator G1 as slack bus without BESS

The scenario with PVs not being able to provide FRT capability is presented first, followed by the scenario with PVs capable of riding through fault, i.e., with FRT.

1) PV systems without FRT capability

A sub-scenario of 30% PV under a 3-phase short circuit is carried out with an assumption that only WT is equipped with FRT functionality. The variation of PV and WT power output is shown in Fig. 4. Due to the lack of FRT capability, all PVs are disconnected by their anti-islanding protection, leaving only WTs connected to the grid over the fault.

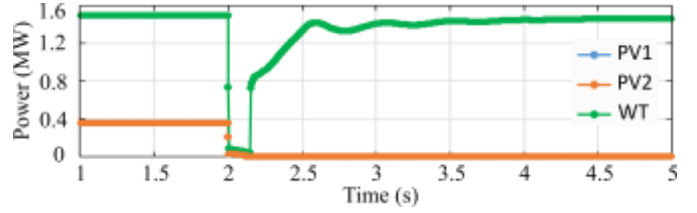


Figure 4. Variation of PVs and WT production.

The variation of the voltage at 22 kV Bus 1 and the grid frequency for different PV levels are shown in Fig. 5 and 6, respectively. As is clear, when the PV level reaches 60%, the frequency goes beyond the permissible range, showing that the grid is unstable after the disturbance. This is because the post-fault power imbalance due to the large disconnection of PVs in 60% scenario exceeds the limit of the two diesel generators G1 (slack) and G2. Besides, the variation of the power outputs of G1 and G2 and their rotor angles for different PV penetrations (0-60%) is shown in Fig. 7 and 8.

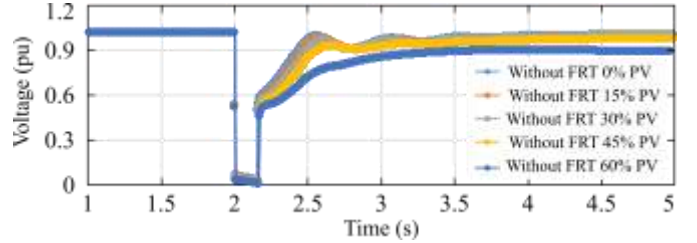


Figure 5. Variation of voltage at Bus 1

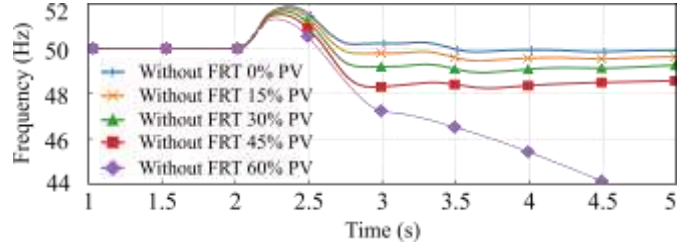


Figure 6. Variation of the frequency

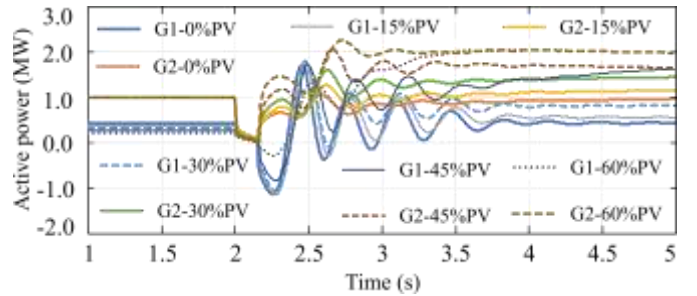


Figure 7. Variation of diesel production

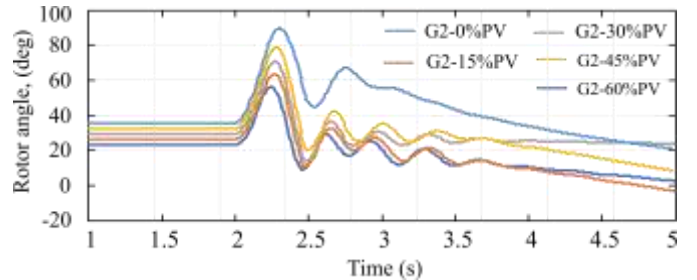


Figure 8. Variation of rotor angle of diesel generators

2) PV systems with FRT capability

A similar three-phase short circuit with all PV and WT systems capable of meeting FRT requirements specified in [16] is considered in this sub-scenario. Fig. 9 depicts the variation of voltage at PV point of common coupling (PCC) against the FRT curve for 60% PV level, proving that all PV and WT systems remain connected to the grid after the fault clearance (Fig. 10). As is evident, in contrast to the previous case, owing to the FRT capability of all PV systems, the grid frequency stabilizes regardless of the PV penetration level as shown in Fig. 11 for 0 to 60% PV level.

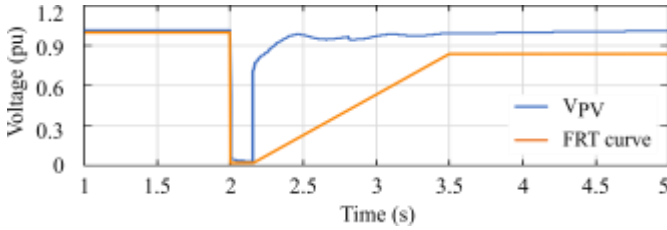


Figure 9. Variation of PV voltage against FRT curve in case of 60% PV

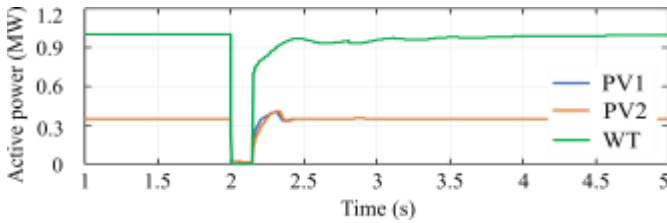


Figure 10. Variation of power output of PV and WT systems (60% PV)

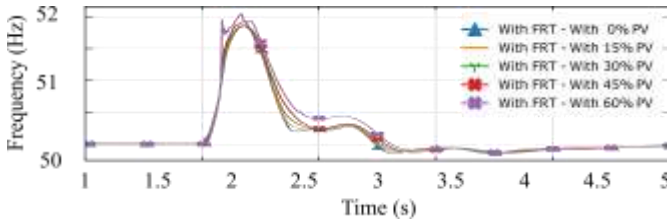


Figure 11. Variation of the frequency

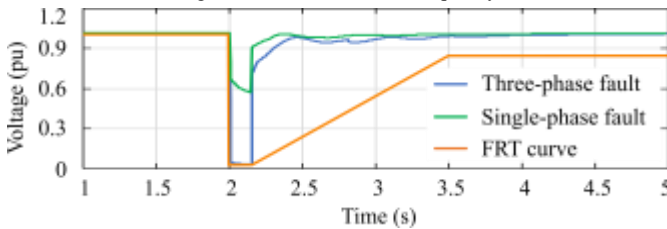


Figure 12. Variation of PV positive-sequence voltage for single and three-phase short-circuit under a 60% PV scenario

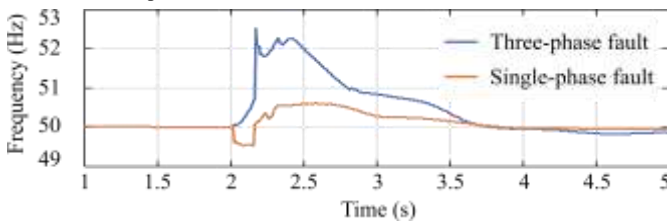


Figure 13. Variation of the frequency for single and three phase-short circuit under a 60% PV scenario

Furthermore, PV response to an unbalanced fault (single-phase short circuit) is also analyzed. The corresponding fluctuations of PV positive-sequence voltage and grid

frequency for the two fault conditions are provided in Fig. 12 and 13, respectively. Similarly, PV and WT systems still show a good operation but the three-phase fault, as always, presents more severe effect with much larger positive-sequence voltage drop and wider frequency variation.

B. Case B: BESS as slack bus

For this scenario, all renewable sources are equipped FRT with WT being operated at 2.75 MW while PV1 and PV2 being at 0.7 MW and 0.9 MW, respectively. Fig. 14 preliminarily presents the variation of the frequency with and without BESS. Obviously, the presence of BESS considerably improves the grid stability.

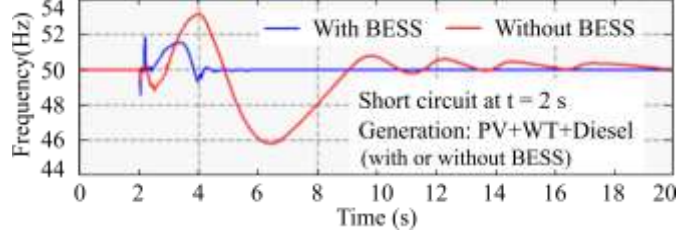


Figure 14. Variation of the frequency in case without and with BESS.

In the following, two disturbances are considered with the first being G1 outage and the second being short-circuit in the grid with 100% inverter-interfaced generation.

1) Outage of diesel generator G1

For this case, G1 is the only synchronous generator being operated and is disconnected at $t=3$ s, leaving the grid fully fed by renewable sources with the production shortage being compensated by BESS as shown in Fig. 15. The variation of PV and WT power outputs also is presented in Fig. 16.

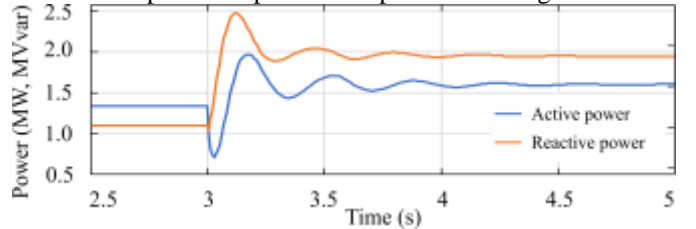


Figure 15. Variation of active and reactive power of BESS

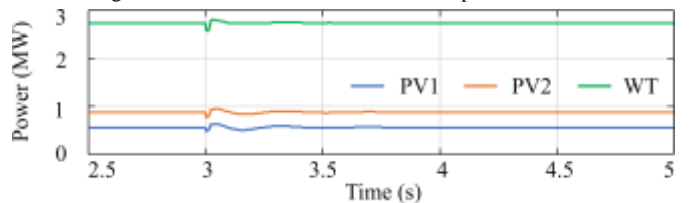


Figure 16. Variation of PV and WT power output

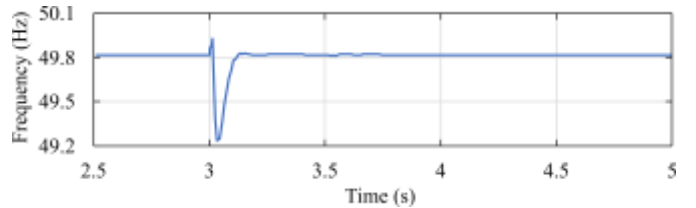


Figure 17. Variation of the frequency

Thanks to the BESS support, the system is stable after the fault isolation with grid frequency being returned to normal

value after a short fluctuation as shown in Fig. 17. Moreover, the BESS also injects additional reactive power to keep the voltage at its PCC closed to 1 pu as demonstrated in Fig. 18.

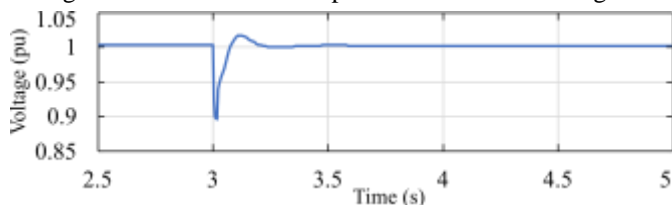


Figure 18. Variation of voltage

2) Short circuit without synchronous machines

Different types of faults are assumed to occur at line segment between Bus 3 and Bus 4 of Feeder 3 at $t=5$ s (Fig. 2) and be eliminated after 0.15 s by the feeder circuit breaker. Fig. 19 presents the variation of power output of PVs and WT for a three-phase short-circuit.

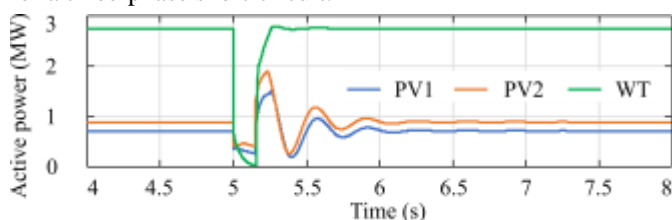


Figure 19. Variation of PV and WT power for three-phase fault

Similar to Case A2, two kinds of fault are carried out to have a comparison of PV and BESS dynamics under different fault conditions. Fig. 20 shows that after several oscillations, BESS attained post-fault stable operation in both scenarios.

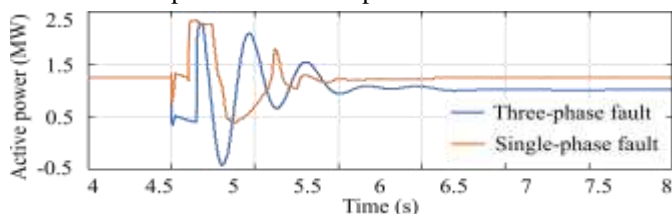


Figure 20. Variation of BESS power output for two fault scenarios

Furthermore, Fig. 21 and 22 illustrate the variation of voltage and frequency for these short-circuit conditions. The grid is still stable for these two fault scenarios, but the three-phase fault shows itself more severe.

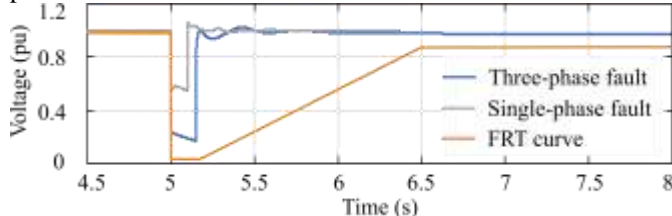


Figure 21. Variation of voltage

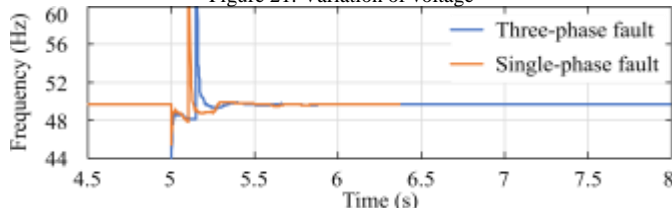


Figure 22. Variation of the frequency for single and three phase short circuit

V. CONCLUSION

In the paper, the authors have conducted a comprehensive study on the transient stability of a real island grid with various scenarios. The results have shown that the FRT capability of the PVs significantly enhances the grid transient stability and thus allows for a higher PV penetration level. On the other hand, the role of BESS in ensuring the stability of the grid fully supplied by only renewable sources is vital. Without BESS support, the grid obviously faces with instability in case of both outage of one diesel generator and short circuit. Lastly, between two fault types studied, the three-phase fault imposes a more severe impact on the grid stability with more considerable variations of voltage and frequency. Evidently, the results derived from this stability assessment provide a clear landscape for the further plan of increasing integration of renewable energy into Con Dao grid.

REFERENCES

- [1] T. Tran-Quoc, C. Andrieu, and N. Hadjsaid, "Technical impacts of small, distributed generation units on LV networks," in *2003 IEEE Power Engineering Society General Meeting (IEEE Cat. No.03CH37491)*, Jul. 2003, vol. 4, pp. 2459-2464 Vol. 4.
- [2] Tran-Quoc *et al.*, "Stability Analysis for the Distribution Networks with Distributed Generation," in *2005/2006 IEEE/PES Transmission and Distribution Conference and Exhibition*, May 2006, pp. 289-294.
- [3] T. Tran-Quoc, *Dynamic analysis of a stand-alone hybrid PV-diesel system with battery storage*. Oct. 2012.
- [4] N. Hatziargyriou, H. Asano, R. Irvani, and C. Marnay, "Microgrids," *IEEE Power and Energy Magazine*, vol. 5, no. 4, pp. 78-94, Jul. 2007.
- [5] R. Majumder, "Some Aspects of Stability in Microgrids," *IEEE Transactions on Power Systems*, vol. 28, pp. 3243-3252, Aug. 2013.
- [6] N. Beg, A. Armstorfer, A. Rosin, and H. Biechl, "Mathematical Modeling and Stability Analysis of a Microgrid in Island Operation," in *2018 International Conference on Smart Energy Systems and Technologies (SEST)*, Sep. 2018, pp. 1-6.
- [7] Y. Song, D. J. Hill, T. Liu, and Y. Zheng, "A Distributed Framework for Stability Evaluation and Enhancement of Inverter-Based Microgrids," *IEEE Transactions on Smart Grid*, vol. 8, no. 6, pp. 3020-3034, Nov. 2017.
- [8] A. Kunwar, F. Shahnia, and R. C. Bansald, "Eigenvalue-Oriented Dynamic Stability Examination to Enhance Designing a Microgrid Hosting Clusters of Inertial and Non-Inertial Distributed Generators," *IEEE Transactions on Smart Grid*, vol. 11, pp. 1942-1955, May 2020.
- [9] D. Choi, J.-W. Park, and S. H. Lee, "Virtual Multi-Slack Droop Control of Stand-Alone Microgrid with High Renewable Penetration Based on Power Sensitivity Analysis," *IEEE Transactions on Power Systems*, vol. 33, no. 3, pp. 3408-3417, May 2018.
- [10] A. Rahmoun, N. Beg, A. Rosin, and H. Biechl, "Stability and eigenvalue sensitivity analysis of a BESS model in a microgrid," in *2018 IEEE International Energy Conference*, Jun. 2018.
- [11] M. T. Muhssin, L. M. Cipcigan, and Z. A. Obaid, "Small Microgrid stability and performance analysis in isolated island," in *2015 50th International Universities Power Engineering Conference*, Sep. 2015.
- [12] A. Mojallal, S. Lotfifard, and S. M. Azimi, "A Nonlinear Supplementary Controller for Transient Response Improvement of Distributed Generations in Micro-Grids," *IEEE Transactions on Sustainable Energy*, vol. 11, no. 1, pp. 489-499, Jan. 2020.
- [13] R. Khezri, A. Mahmoudi, and S. Golshannavaz, "An Intelligent Fuzzy Control Approach for a Back-Pressure Autonomous Industrial Microgrid," in *2020 IEEE Energy Conversion Congress and Exposition (ECCE)*, Oct. 2020, pp. 2439-2444.
- [14] S. Teimourzadeh, M. Davarpanah, F. Aminifar, and M. Shahidepour, "An Adaptive Auto-Reclosing Scheme to Preserve Transient Stability of Microgrids," *IEEE Transactions on Smart Grid*, vol. 9, no. 4, pp. 2638-2646, Jul. 2018.
- [15] M. Eskandari and A. V. Savkin, "On the Impact of Fault Ride-Through on Transient Stability of Autonomous Microgrids: Nonlinear Analysis and Solution," *IEEE Transactions on Smart Grid*, vol. 12, no. 2, pp. 999-1010, Mar. 2021.
- [16] ERDF-NOI-RES_13E, "Protections des installations de production raccordées au réseau public de distribution Identification", June 2020. Online: Available at: <https://eenedis.fr/site/defaults/files>.